

Incoherent topological defect recombination dynamics in TbTe_3

T. Mertelj¹, P. Kusar¹, V. V. Kabanov¹, I. Fisher^{2,3} and D. Mihailovic^{1,4}

¹*Complex Matter Department, Jozef Stefan Institute, Jamova 39, 1000 Ljubljana, Slovenia*

²*Geballe Laboratory for Advanced Materials and Department of Applied Physics, Stanford University, Stanford, California 94305, USA*

³*Stanford Institute for Materials and Energy Sciences, SLAC National Accelerator Laboratory, 2575 Sand Hill Road, Menlo Park, California 94025, USA and*

⁴*CENN Nanocentre, Jamova 39, 1000 Ljubljana, Slovenia*

(Dated: October 15, 2018)

We study the incoherent recombination of topological defects created during a rapid quench of a charge-density-wave system through the electronic ordering transition. Using a specially devised 3-pulse femtosecond optical spectroscopy technique we follow the evolution of the order parameter over a wide range of timescales. By careful consideration of thermal processes we can clearly identify intrinsic topological defect annihilation processes on a timescale ~ 30 ps and find a signature of extrinsic defect-dominated relaxation dynamics occurring on longer timescales.

PACS numbers: 71.45.Lr, 78.47.jh, 63.20.kp

Topological defects are non-linear objects which can be created any time a symmetry-breaking transition occurs.[1–3] They can be described theoretically as solutions to systems of nonlinear differential equations based on Ginzburg-Landau theory. They are of great fundamental importance in fields such as cosmology where they appear as strings and condensed matter physics where they appear in the form of vortices and domain walls. While a good understanding of static properties of topological defects (TD) has come from systems such as liquid crystals, the dynamics of TDs are much less understood. Electronic phase transitions in charge-density wave systems[4] are particularly interesting model systems for studying the general behavior of the dynamics of topological excitations. The collective excitations are not overdamped which allows the observation of both collective and quasiparticle (QP) excitations as they evolve through the transition. In particular, they can be used to investigate the dynamic behavior of topological excitations such as domain walls in real time using ultrafast laser techniques.

Recently, time-resolved experiments have shown that following a quench created by a strong laser pulse the order parameter (OP) oscillates coherently, revealing coherent TD dynamics.[5] Domain walls are created parallel to the crystal surface which can coherently annihilate on the timescale of a few picoseconds with the accompanying emission of collective modes which have been detected as modulations of reflectivity upon reaching the surface. In addition to coherent defect dynamics, incoherent topological defects created by the Kibble-Zurek mechanism[2] are also expected, but very little is known about the dynamics of incoherent TD dynamics in CDW systems, and in condensed matter systems in general.

In this paper we investigate the incoherent evolution of TDs using a specially devised 3-pulse femtosecond spectroscopy[5] technique which allows the direct background free observation of the evolution of the order parameter (OP) as a function of time through the electronic ordering transition. In a rapid quench experiment

order emerges in different regions of the sample independently so multiple topological defects can be created. Their presence can be detected in the optical response as a spatial inhomogeneity of the order parameter. The determination of incoherent TD dynamics is a challenging task, however. Because of thermal diffusion processes, which evolve on similar timescales as topological annihilation and also introduce temperature inhomogeneity, careful temperature calibration from independently measured frequencies is needed to accurately account for thermal effects. We deal with the problem by careful calibration of the transient effective temperatures, which enables us to unambiguously distinguish the incoherent dynamics from thermal diffusion effects.

In our experiments, we use a three pulse technique described in refs. [5, 6]: A "destruction" (D) laser pulse at 800 nm excites a cold sample[17] into the disordered state, breaking up the CDW order. We then monitor the evolution of the transient reflectivity $\Delta R(t_{\text{DP}})/R$ excited with a weaker pump (P) pulse as a function of time delay t_{DP} between the D and P pulse (the pulse sequence nomenclature is illustrated in the insert to Fig. 1b)). The D pulse fluence is adjusted to twice the threshold for causing the destruction of the ordered state [5]. After a quench by the laser pulse, order recovers first through the sub-picosecond recovery of the quasiparticle gap leading to coherent oscillations of the OP and the coherent creation of TDs which decay within 5-8 ps in TbTe_3 [5]. Since the CDW coherence length (~ 2 nm) is much shorter than the size of the laser excited volume ($\sim 50\mu\text{m}$ dia), order emerges with different phase in different regions, resulting in the formation of topological defects whose spatial distribution is determined partly by the inhomogeneous excitation and partly by the underlying fluctuations which nucleate the emergence of order by the so called Kibble-Zurek[2, 3] mechanism. The resulting inhomogeneity of the OP leads to observable temporally resolvable effects in the frequency, linewidth and amplitude of the collective amplitude mode, all of which

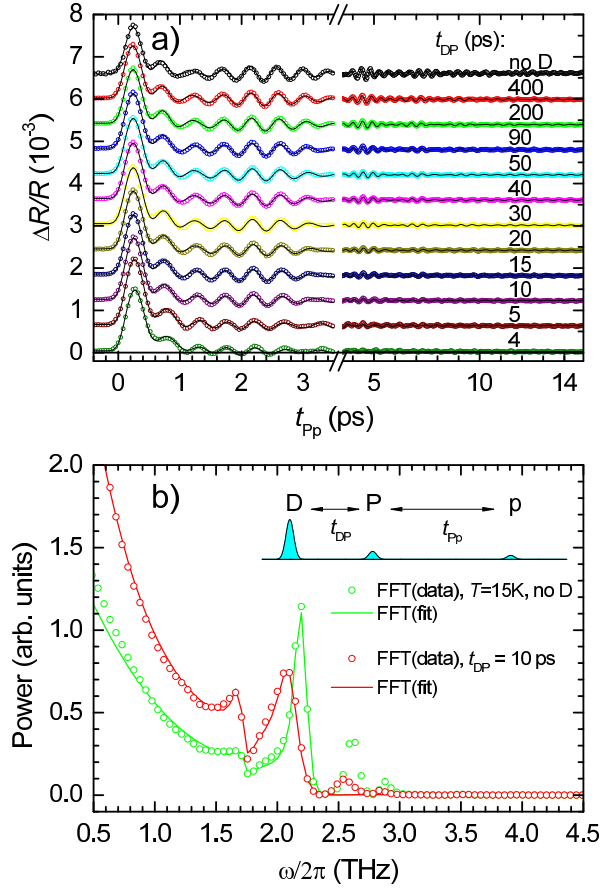


Figure 1: a) The transient reflectivity of TbTe₃ at different times t_{DP} after the D pulse. The thin lines are the fits discussed in text. b) An example of the FFT power spectra for the raw data and the fit at $t_{DP} = 10$ ps with and without a D pulse. The inset shows the laser pulse sequence.

are related to the OP, as shown in previous studies[7].

In Fig. 1(a) we show the raw data on the transient reflectivity $\Delta R(t_{DP})/R$ of TbTe₃ at different time delays t_{DP} after the D pulse. After the initial QP relaxation we observe oscillations due to the coherently excited order parameter amplitude mode (AM) and other phonons.[7, 9, 10] The level of noise is very small, due to the excellent intrinsic properties of the material, which helps us make a detailed quantitative analysis. We analyze the transient reflectivity oscillations using the theory for displacive excitation of coherent phonons:[11]

$$\frac{\Delta R(t_{DP})}{R} = \int_0^\infty G(t-u) \times [A_e \exp(-u/\tau) + A_B] du + \sum A_i \int_0^\infty G(t-u) \exp(-\gamma_i u) \times [\cos(\Omega_i u) - \beta_i \sin(\Omega_i u)] du \quad (1)$$

where $\beta_i = (1/\tau - \gamma_i)/\Omega_i$, $G(t) = \exp(-2t^2/\tau_p^2)$ and τ_p is the laser pulse length. The first integral represents the

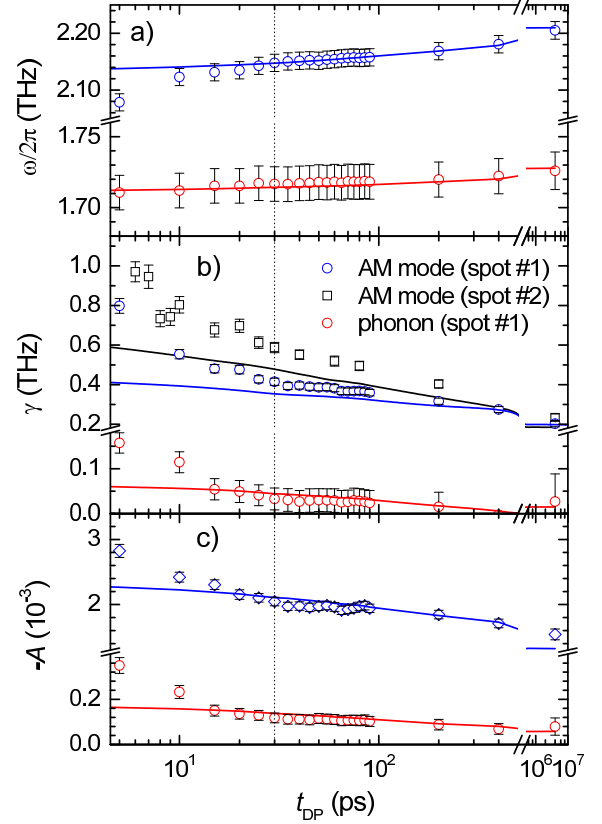


Figure 2: a) Frequencies of the AM and the 1.7-THz phonon as a function of t_{DP} . b) Effective dampings of the AM and the phonon as a function of t_{DP} . Open squares represent a measurement from another spot on the sample. c) Amplitudes of the AM and the phonon as a function of t_{DP} . The solid lines are the frequencies, linewidths and amplitudes calculated using an inhomogeneous temperature distribution model.[8] Since no special care was taken to calibrate the D-pulse beam diameter at the sample for the measurement on spot #2 the actual D-pulse fluence on spot #2 was slightly higher leading to different TDM parameters.

QP relaxation with the relaxation time τ , while the sum depicts the response of coherent phonons with frequencies Ω_i , and effective dampings γ_i . A_e corresponds to the QP relaxation amplitude while the residual value at long delays is A_B . To limit the number of fitting parameters we keep only two phonon terms corresponding to the AM at 2.2 THz and the 1.7-THz phonon which strongly interacts with the AM at higher temperatures.[7] Fig 1(b) shows the fast Fourier transform (FFT) of the raw data and of the fit to the data i) without the D pulse and ii) for a D-P delay of $t_{DP} = 10$ ps, clearly showing that Eq. (1) fits the response very well below ~ 2.4 THz irrespective of t_{DP} . The t_{DP} -dependence of the frequency, linewidth and amplitude of the AM and 1.7 THz phonon modes are shown in Fig. 2. The linewidth is shown for two sets of

data obtained from different spots on the sample in two separate measurements.

In order to obtain a calibration of the effective temperature T_{eff} of the photoexcited sample volume we measured *independently*, by means of a standard pump-probe experiment, the T -dependence of the reflectivity transients in the thermal equilibrium and determine the T -dependent amplitude, frequency $[\omega_{\text{AM}}(T)]$ and damping $[\gamma_{\text{AM}}(T)]$ for the AM. Using these calibrations we are in a position to determine T_{eff} as a function of time from $\omega_{\text{AM}}(t_{\text{DP}})$ and $\gamma_{\text{AM}}(t_{\text{DP}})$ and take it into account to obtain the thermal inhomogeneity dynamics. The time-dependence of the T_{eff} is shown in Fig. 3(b). We observe that the two effective temperatures $T_{\omega}(t_{\text{DP}})$ and $T_{\gamma}(t_{\text{DP}})$ obtained from the $\omega_{\text{AM}}(t_{\text{DP}})$ and $\gamma_{\text{AM}}(t_{\text{DP}})$ systematically differ by approximately 20 K indicating an excess AM linewidth with respect to the thermal equilibrium state.

One of the most obvious contributions to the excess AM linewidth is the inhomogeneous broadening caused by the thermal inhomogeneity. In order to be able to determine and analyze any other contributions to the linewidth we therefore determine the contribution of the thermal inhomogeneity to the excess AM linewidth. To do this we first fit a thermal diffusion model[8, 12] (TDM) to the effective temperature obtained from the AM frequency $T_{\omega}(t_{\text{DP}})$, and then use the TDM parameters to calculate the transient optical reflectivity which fully takes into account inhomogeneity of the temperature in the excited volume.[8] As seen in Fig. 3 (b), $T_{\omega}(t_{\text{DP}})$ can be fit very well over 5 decades of time from 30 ps to 4 μs using a one-dimensional[18] TDM, where $T(t_{\text{DP}}) = \Delta T / \sqrt{1 + t_{\text{DP}}/\tau_{\text{D}}} + T_0$, and the fit parameter $\tau_{\text{D}} \sim 120$ ps represents the characteristic heat diffusion time[8].

Comparing now the simulation[8] with the experiment in Fig. 2, we see that the validity of the TDM beyond ~ 30 ps is well supported by the good agreement of the simulation for both the AM and the 1.7-THz phonon parameters. We can thus safely conclude, that the recovery of the order parameter on timescales longer than ~ 30 ps is primarily governed by the 1D heat diffusion process.

Below ~ 30 ps however, there is a large discrepancy between the calculated T_{eff} , γ_{AM} and other phonon parameters in comparison to the data, even after carefully taking into account the thermal inhomogeneity. The observed magnitude and the evolution of $\gamma_{\text{AM}}(t_{\text{DP}})$ for $t_{\text{DP}} < 30$ ps clearly cannot be assigned solely to the temperature inhomogeneity. Subtracting the thermal inhomogeneity contribution from the AM linewidth in Fig. 2 b), we can now isolate the topological-defects inhomogeneity contribution as shown in Fig. 4.

As discussed in the introduction some of the defects created in the quench process annihilate *coherently* resulting in an aperiodic modulation of the AM intensity and frequency in the first ~ 8 picoseconds[5]. The very low level of experimental noise in the raw data allows us to attribute the observed data scatter in Fig. 4 to the

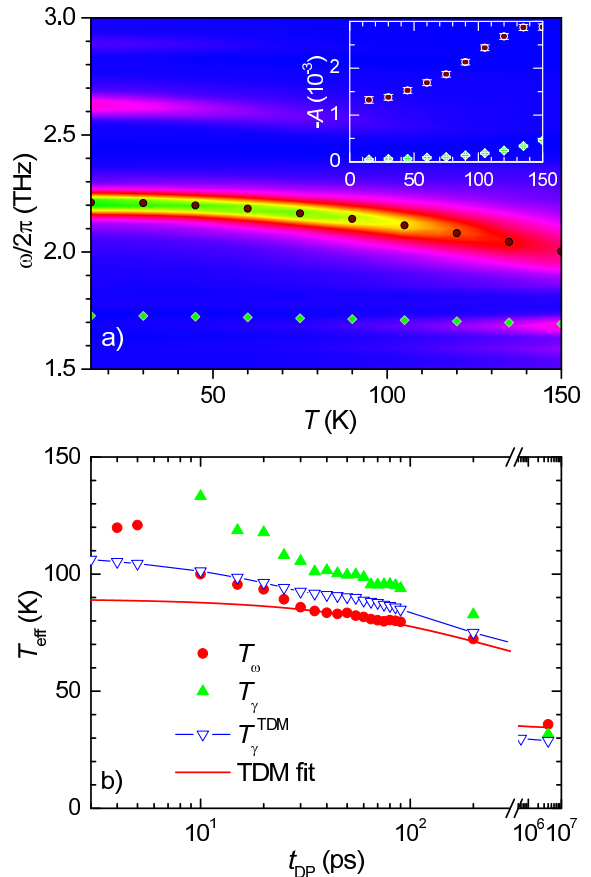


Figure 3: a) The temperature dependence of the coherent oscillations spectrum measured in a standard Pp experiment. Circles and diamonds represent the frequencies obtained from the time domain fit for the AM and the 1.7-THz phonon, respectively. The inset shows the T -dependence of the amplitudes for both modes. b) The time-dependence of the effective temperature $T_{\text{eff}}(t_{\text{DP}})$ from $\omega_{\text{AM}}(t_{\text{DP}})$ and $\gamma_{\text{AM}}(t_{\text{DP}})$. The solid line is a fit to ω_{AM} effective temperature using the thermal diffusion model. The inverted triangles correspond to the calculated $T_{\gamma}^{\text{TDM}}(t_{\text{DP}})$ taking into account the inhomogeneous temperature distribution.[8]

coherent defect dynamics in the material, rather than experimental noise.

The modulation of the AM due to the defects that annihilate *incoherently* is unfortunately not detected *directly* by our stroboscopic technique. However, the incoherent topological defects give rise to a spatial inhomogeneity of the order parameter and a *decoherence* of the AM oscillations leading to an increased linewidth γ_{AM} for $t_{\text{DP}} < 30$ ps which we have detected in our experiments. Concurrently the defects give rise to a softening of the collective mode ω_{AM} , because of the OP suppression which they cause. The increase of the coupled 1.7-THz phonon effective damping at shorter t_{DP} as shown in Fig. 2 is presumably also caused by the inhomogeneity of the OP. A further manifestation of the incoherent annihila-

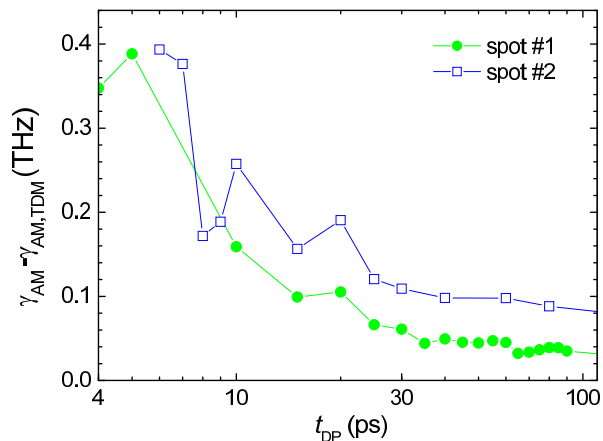


Figure 4: The time-dependence of the excess γ_{AM} due to topological defect annihilation. Data for two different spots on the sample show a difference primarily in the long time behavior beyond 30 ps, which appears as an offset.[13]

tion is the increase of the amplitudes of the AM and the phonon with respect to the TDM for $t_{DP} < \sim 30$ ps, which is also consistent with the suppression of the OP when one takes into account that the amplitudes of the modes increase with the decreasing OP amplitude deduced from their T -dependence shown in the inset of Fig. 3(a).

Apart from intrinsic topological defect annihilation processes, which we have identified on a timescale of ~ 30 ps, we expect to observe annihilation of domain walls pinned to defects and imperfections at longer times. The timescale of their annihilation may extend well beyond 30 ps. Evidence for such slower extrinsic recombination processes comes from the long time behavior shown in Fig.

4. γ_{AM} remains systematically larger than the predicted thermally inhomogeneous linewidth γ_{AM}^{TDM} suggesting a slower recombination of the pinned domain walls.[13]

Recently the absence of topological defects on ultrafast timescales in highly excited charge ordered (CO) nickelate was suggested.[14] A slow relaxation of the CO X-ray diffraction peak intensity, on the timescale of ~ 60 ps, was, due to the absence of any increase of the diffraction peak linewidth, attributed to a depopulation of the phason mode. While, contrary to Lee et al. [14], our excitation density is clearly high enough to excite topological defects,[5] there exists a possible anharmonic contribution of the highly excited phason mode to the AM linewidth. The anharmonic processes, however, contribute to both, the linewidth and frequency renormalization of the AM,[15] and *can not* lead to the difference between T_ω and T_γ as observed in the experiment.

In conclusion, these experiments demonstrate the possibility of studying both coherent and incoherent topological defects dynamics in complex materials in which the order parameter can be monitored in real time through the dynamics of the collective mode. The dynamics on a timescale of ~ 30 ps can unambiguously be associated with intrinsic topological defects annihilation in $TbTe_3$ following a laser quench arising from the time-dependent inhomogeneity and suppression of the order parameter. The inhomogeneity causes an increased effective damping of the amplitude mode while the suppression of the order-parameter is indicated by an additional softening of the AM-mode frequency. Beyond ~ 30 ps we find a predominantly thermal-diffusion governed order-parameter dynamics with a signature of extrinsic defect annihilation dynamics.

-
- [1] Y. Bunkov and H. Godfrin, *Topological defects and the non-equilibrium dynamics of symmetry breaking phase transitions*, vol. 549 (Springer, 2000).
- [2] T. W. B. Kibble, *Journal of Physics A: Mathematical and General* **9**, 1387 (1976), URL <http://stacks.iop.org/0305-4470/9/i=8/a=029>.
- [3] W. Zurek, *Nature* **317**, 505 (1985).
- [4] G. Grüner, *Density waves in solids* (Addison-Wesley New York, 1994).
- [5] R. V. Yusupov, T. Mertelj, P. Kucar, V. Kabanov, S. Brazovskii, J.-H. Chu, I. R. Fisher, and D. Mihailovic, *Nature Physics* **6**, 681 (2010).
- [6] P. Kucar, T. Mertelj, V. V. Kabanov, J.-H. Chu, I. R. Fisher, H. Berger, L. Forró, and D. Mihailovic, *Phys. Rev. B* **83**, 035104 (2011), URL <http://link.aps.org/doi/10.1103/PhysRevB.83.035104>.
- [7] R. V. Yusupov, T. Mertelj, J.-H. Chu, I. R. Fisher, and D. Mihailovic, *Phys. Rev. Lett.* **101**, 246402 (2008), URL <http://link.aps.org/doi/10.1103/PhysRevLett.101.246402>.
- [8] Please see supplemental information.
- [9] F. Schmitt, P. Kirchmann, U. Bovensiepen, R. Moore, L. Rettig, M. Krenz, J. Chu, N. Ru, L. Perfetti, D. Lu, et al., *Science* **321**, 1649 (2008).
- [10] M. Lavagnini, H.-M. Eiter, L. Tassini, B. Muschler, R. Hackl, R. Monnier, J.-H. Chu, I. R. Fisher, and L. Degiorgi, *Phys. Rev. B* **81**, 081101 (2010), URL <http://link.aps.org/doi/10.1103/PhysRevB.81.081101>.
- [11] H. J. Zeiger, J. Vidal, T. K. Cheng, E. P. Ippen, G. Dresselhaus, and M. S. Dresselhaus, *Phys. Rev. B* **45**, 768 (1992), URL <http://link.aps.org/doi/10.1103/PhysRevB.45.768>.
- [12] T. Mertelj, A. Ošlak, J. Dolinšek, I. R. Fisher, V. V. Kabanov, and D. Mihailovic, *Phys. Rev. Lett.* **102**, 086405 (2009), URL <http://link.aps.org/doi/10.1103/PhysRevLett.102.086405>.
- [13] In the standard 2-pulse pump-probe experiments we observe some spatial variation of the AM linewidth which we assign to the intrinsic structural-defect/impurity density spatial variation in the sample. Since, in the absence of 2-pulse T -dependent data for spot #2, the TDM simulation for spot #2 was based on T -dependent scans from spot #1 the offset between the spots can be attributed to the systematic error due to the spatial variation of the AM linewidth.
- [14] W. Lee, Y. Chuang, R. Moore, Y. Zhu, L. Patthey, M. Trigo, D. Lu, P. Kirchmann, O. Krupin, M. Yi, et al.,

- Nature Communications **3**, 838 (2012).
- [15] M. Balkanski, R. F. Wallis, and E. Haro, Phys. Rev. B **28**, 1928 (1983), URL <http://link.aps.org/doi/10.1103/PhysRevB.28.1928>.
- [16] N. Ru, C. Condrón, G. Margulis, K. Shin, J. Laverock, S. Dugdale, M. Toney, and I. Fisher, Physical Review B **77**, 035114 (2008).
- [17] The growth of the samples by a self-flux technique and subsequent characterization was described elsewhere.[16]
- [18] The diameters of the beams are much larger than the optical penetration depth so on the relevant timescale the heat diffusion is 1D.

Incoherent topological defect recombination dynamics in TbTe₃: supplemental information

T. Mertelj¹, P. Kusar¹, V. V. Kabanov¹, I. Fisher^{2,3} and D. Mihailovic^{1,4}

¹Complex Matter Department, Jozef Stefan Institute, Jamova 39, 1000 Ljubljana, Slovenia

²Geballe Laboratory for Advanced Materials and Department of Applied Physics, Stanford University, Stanford, California 94305, USA

³Stanford Institute for Materials and Energy Sciences, SLAC National Accelerator Laboratory, 2575 Sand Hill Road, Menlo Park, California 94025, USA and

⁴CENN Nanocentre, Jamova 39, 1000 Ljubljana, Slovenia

(Dated: October 15, 2018)

I. THERMAL DIFFUSION MODEL SIMULATION

A. Temperature inhomogeneity

On longer time scales, when the system is locally thermalized, it can be described by the microscopical thermodynamic temperature, which is governed by the heat-diffusion equation, $\frac{\partial T}{\partial t} = D(T)\nabla^2 T$. Due to the experimental geometry, where the experimental volume has a shape of a high aspect ratio pancake, with the diameter much larger than the thickness, the diffusion is one dimensional (1D) on all relevant timescales.

The 1D solution of the heat-diffusion equation, using the von Neumann boundary condition, $\frac{\partial T(t,z)}{\partial z} = 0$, at $z = 0$ and assuming a T independent diffusion constant D , is:

$$\Delta T = \frac{1}{\sqrt{4\pi Dt}} \int_0^\infty \left(e^{-\frac{(z-u)^2}{4Dt}} + e^{-\frac{(z+u)^2}{4Dt}} \right) \Delta T(0, u) du. \quad (\text{S1})$$

When the initial temperature $\Delta T(0, z)$ is given by the exponentially decaying laser pulse depth profile, $\Delta T(0, z) = \Delta T \exp(-z/\lambda_p)$, with λ_p being the optical penetration depth in units of the correlation length and ΔT a positive coefficient depending on the intensity of the pulse, we obtain the solution:

$$\begin{aligned} \Delta T(t, z) = & \frac{\Delta T}{2} e^{t/4\tau_D} \cdot \\ & \left[e^{-z/\lambda_p} \operatorname{erfc} \left(\sqrt{\frac{t}{4\tau_D}} - \frac{z}{\lambda_p} \sqrt{\frac{\tau_D}{t}} \right) + \right. \\ & \left. + e^{z/\lambda_p} \operatorname{erfc} \left(\sqrt{\frac{t}{4\tau_D}} + \frac{z}{\lambda_p} \sqrt{\frac{\tau_D}{t}} \right) \right]. \quad (\text{S2}) \end{aligned}$$

Here $\tau_D = \lambda_p^2/4D$ is the characteristic heat diffusion time. A simpler solution is found using the initial temperature $\Delta T(0, z)$ with a Gaussian profile[1] $\Delta T_G(0, z) = \Delta T \exp(-z^2/\lambda_p^2)$,

$$\Delta T_G(t, z) = \frac{\Delta T}{\sqrt{(1+t/\tau_D)}} \exp\left(-\frac{z^2}{\lambda_p^2(1+t/\tau_D)}\right). \quad (\text{S3})$$

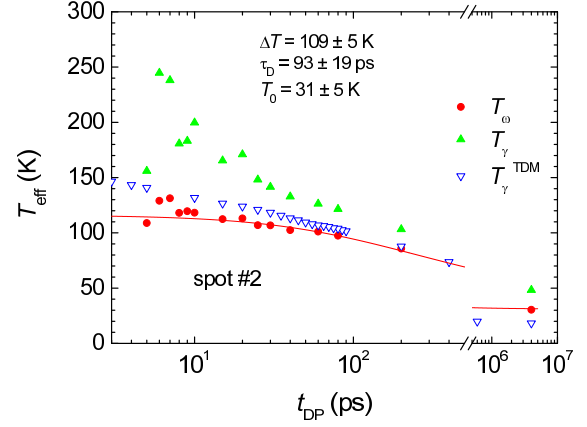


Figure S1: The time-dependence of the effective temperature $T_{\text{eff}}(t_{\text{DP}})$ obtained from $\omega_{\text{AM}}(t_{\text{DP}})$ and $\gamma_{\text{AM}}(t_{\text{DP}})$ at spot #2. The solid line is a fit to ω_{AM} effective temperature using the thermal diffusion model (S3). The inverted triangles correspond to the calculated $T_{\gamma}^{\text{TDM}}(t_{\text{DP}})$ taking into account the inhomogeneous temperature distribution. The underestimation of T_{γ}^{TDM} at long t_{DP} is due to the intrinsic variation of the thermal equilibrium γ_{AM} . [2]

B. Optical reflectivity transients in the presence of the temperature inhomogeneity

To calculate the excess AM linewidth due to the inhomogeneous broadening caused by the thermal inhomogeneity we first fit a thermal diffusion model (S3) (TDM) to the effective temperature obtained from the AM frequency, $T_{\omega}(t_{\text{DP}})$. As seen in Fig. 3(b) and S1, $T_{\omega}(t_{\text{DP}})$ can be fit very well over 5 decades of time from 30 ps to 4 μs .

Next we simulate the optical reflectivity response in the presence of the inhomogeneous temperature distribution using the thermal diffusion parameters obtained from the

fit above. The response is given by:

$$\frac{\Delta R_{\text{TDM}}(t_{\text{PP}})}{R} \Big|_{t_{\text{DP}}} = \int_0^\infty e^{-3z/\lambda_{\text{op}}} \times \frac{\Delta R(t_{\text{PP}})}{R} \Big|_{T(z,t_{\text{DP}})} dz \quad (\text{S4})$$

$$T(z, t_{\text{DP}}) = \Delta T(t_{\text{DP}}, z) + T_0. \quad (\text{S5})$$

Here λ_{op} is the optical penetration depth and

$\Delta R(t_{\text{PP}})/R|_{T(t_{\text{DP}},z)}$ in (S4) is calculated by interpolation from the T -dependent transients which were independently measured in the thermal equilibrium. From the calculated response in Eq. (S4) we then determine the predicted thermally inhomogeneous linewidth $\gamma_{\text{AM}}^{\text{TDM}}(t_{\text{DP}})$, and other phonon parameters, as well as the effective temperature $T_\gamma^{\text{TDM}}(t_{\text{DP}})$ in the same way as previously, by fitting Eq. (1).

-
- [1] T. Mertelj, A. Ošlak, J. Dolinšek, I. R. Fisher, V. V. Kabanov, and D. Mihailovic, Phys. Rev. Lett. **102**, 086405 (2009), URL <http://link.aps.org/doi/10.1103/PhysRevLett.102.086405>.
- [2] In the standard 2-pulse pump-probe experiments we observe some spatial variation of the AM linewidth which we assign to the intrinsic structural-defect/impurity density spatial variation in the sample. In the absence of 2-pulse T -dependent data for spot #2 the TDM simulation for spot #2 was based on T -dependent scans from spot #1. This lead to the systematic error due to the spatial variation of the AM linewidth.